

Probing the full distribution of many-body observables by single-qubit interferometry

Zhenyu Xu^{1,2} and Adolfo del Campo^{2,3}

¹*School of Physical Science and Technology, Soochow University, Suzhou 215006, China*

²*Department of Physics, University of Massachusetts, Boston, MA 02125, USA*

³*Theoretical Division, Los Alamos National Laboratory, Los Alamos, NM 87545, USA*

We present an experimental scheme to measure the full distribution of many-body observables in spin systems, both in and out of equilibrium, using an auxiliary qubit as a probe. We focus on the determination of the magnetization and the kink-number statistics at thermal equilibrium. The corresponding characteristic functions are related to the analytically-continued partition function. Thus, both distributions can be directly extracted from experimental measurements of the coherence of a probe qubit that is coupled to an Ising-type bath, as reported in [X. Peng, Phys. Rev. Lett. **114**, 010601 (2015)] for the detection of Lee-Yang zeroes.

Across a continuous phase transition, a system evolves from a high-symmetry phase to a broken symmetry phase characterized by the emergence of a new macroscopic order. The latter can be detected by the order parameter, which vanishes in the high-symmetry phase and acquires a non-zero value below the critical point. A paradigmatic example is the transition between a paramagnet and a ferromagnet in spin systems, in which the magnetization is the order parameter.

The characterization of the order parameter statistics beyond its mean value is motivated both by the possibility to probe its fluctuations and the quest for the fundamental physics they may unveil, both in and out of equilibrium. Pioneering studies in spin systems [1–4] focused on the distribution of the magnetization. The latter has applications in a wide variety of contexts ranging from the characterization of density fluctuations in a liquid-gas critical point [5] to the study of turbulent fluids [6, 7]. The distribution of other many-body observables in spin systems has also proved useful. A prominent example is the number distribution of topological defects, that is relevant to memory devices and magnetic data storage [8, 9] and the study of universal critical dynamics beyond the paradigmatic Kibble-Zurek mechanism [10, 11]. Measuring the full distribution of many-body observables in the laboratory is however a challenging task.

An auxiliary system, such as a single qubit, can be used as a meter in this context. In particular, single-qubit interferometry has been used to characterize quantum fluids [12–14], determine Loschmidt echoes [15–18], monitor critical dynamics of decoherence [19], measure work statistics [20–23], the temperature of a sample [24], out-of-time order correlators [25, 26], and the distribution of Lee-Yang zeroes [27–29], to name some relevant examples.

In this work, we propose an experimental protocol to measure the full distribution of a wide class of many-body observables in a spin system making use of a single auxiliary probe qubit. In particular, we focus on the determination of the magnetization and kink-number distributions. To this end, we first show that the corresponding

characteristic functions at equilibrium are given by the analytic continuation of the partition function in classical systems. Exploiting this connection, we show that the probability distributions can be experimentally measured (e.g. in a NMR setting) by monitoring the quantum coherence of the probe qubit that is coupled to the spin bath, that has already been demonstrated in the laboratory [27–29].

Statistics of many-body observables.— Consider a system of N interacting spins subject to a magnetic field h and described by the Hamiltonian

$$H_s(\mathcal{J}, h) = - \sum_{l=1}^N \sum_{n_1 < \dots < n_l} J_{n_1 \dots n_l} \sigma_{n_1} \dots \sigma_{n_l} - h \sum_{n=1}^N \sigma_n, \quad (1)$$

where the spin σ takes values ± 1 and the first term describes arbitrary interactions among spins, including onsite disorder. The equilibrium properties of such system can be extracted with knowledge of the partition function in the canonical ensemble $Z(\mathcal{J}, h, \beta) = \sum_{\{\sigma=\pm 1\}} e^{-\beta H_s(\mathcal{J}, h)}$, where \mathcal{J} denotes the set of coupling constants $\{J_{n_1 \dots n_l}\}$, and $\beta = 1/(kT)$. A prominent instance is the Ising chain, where the spin-spin interactions are pair-wise and restricted to nearest neighbors, i.e., $J_{nm} = J\delta_{n,n+1}$ [30, 31]. The latter exhibits a phase transition between a paramagnetic and a ferromagnetic phase, where the new macroscopic order in the broken symmetry phase is detected by the magnetization, that is the order parameter,

$$M = \sum_{n=1}^N \sigma_n, \quad (2)$$

with possible integer values $m \in [-N, N]$. Another example concerns the characterization of domains separated by topological defects, e.g., kinks. The kink number is given by

$$K = \frac{1}{2} \left(N - \sum_{n=1}^N \sigma_n \sigma_{n+1} \right), \quad (3)$$

with possible integer values $k \in [0, N]$. Without loss of generality, in what follows we consider a many-body

observable of the form

$$X = a + b \sum_{\{n_1, \dots, n_l\}} \sigma_{n_1} \cdots \sigma_{n_l}, \quad (4)$$

which includes the magnetization M (with $a = 0$, $b = 1$, $l = 1$) as well as the kink number K with $a = N/2$, $b = -1/2$, $l = 2$ ($\{n_1, n_2\} = \{n, n+1\}$). In this paper, we aim at reconstructing the probability distribution $P(x)$ of X in systems described by Hamiltonian Eq. (1), this is,

$$P(x) = \langle \delta(X - x) \rangle. \quad (5)$$

Here, the average denoted by $\langle \cdot \rangle = \sum_{\{\sigma=\pm 1\}} \rho \cdot$, is taken with respect to the system probability distribution ρ . The Kronecker delta $\delta(x)$ is used, assuming that for a given spin-configuration the statistical quantity X takes integer values $\{x\}$ (in the continuous case a Dirac delta function should be used instead). By using its integral representation, the distribution of $P(x)$ can be expressed as the Fourier transform

$$P(x) = \frac{1}{2\pi} \int_0^{2\pi} d\theta F(\theta) e^{-ix\theta} \quad (6)$$

of the characteristic function

$$F(\theta) = \langle e^{i\theta X} \rangle. \quad (7)$$

At equilibrium, the average is taken with respect to the canonical distribution $\rho_{\text{th}} = e^{-\beta H_s(\mathcal{J}, h)} / Z(\mathcal{J}, h, \beta)$. The characteristic function $F(\theta)$ of $P(x)$ is then given by the analytic continuation of the partition function

$$F(\theta) = e^{i\theta a} \frac{Z(\tilde{\mathcal{J}}, \tilde{h}, \beta)}{Z(\mathcal{J}, h, \beta)}, \quad (8)$$

where $Z(\tilde{\mathcal{J}}, \tilde{h}, \beta) = \sum_{\{\sigma=\pm 1\}} e^{-\beta H_s(\mathcal{J}, h)} e^{i\theta(X-a)}$. Here we have introduced the effective modified set of complex-valued coupling constants $\tilde{\mathcal{J}}$, and the complex magnetic field \tilde{h} , whose explicit forms are related to the specific statistical quantity to be measured, as we detail below.

We note that the analytic continuation of the partition function has proved useful in a variety of contexts including the study of phase transitions [32, 33] and the measurement of Lee-Yang zeros [27–29], as well as the characterization of quantum chaotic systems in relation to information scrambling [34–36] and work statistics [37], among other examples.

Probing the characteristic function with an auxiliary qubit.— A schematic diagram for the detection of characteristic functions with an auxiliary qubit is shown in Fig. 1. The proposed experimental protocol consists of the following steps:

Step 1: The probe qubit is first prepared in the quantum superposition state $|+\rangle = (|\downarrow\rangle + |\uparrow\rangle)/\sqrt{2}$ by the action of a Hadamard gate $H = (\hat{\sigma}_x + \hat{\sigma}_z)/\sqrt{2}$ ($\hat{\sigma}_{x,y,z}$ stand

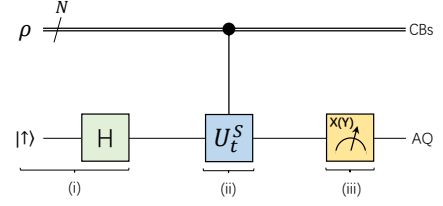


FIG. 1. Scheme for probing the characteristic function of statistical quantity X by a quantum simulator. (i) Initial state preparations. The classical spin (bit) systems (CBs) and the auxiliary qubit (AQ) are prepared respectively in probability distribution ρ (or a thermal equilibrium state ρ_{th} discussed in the main text), and a superposition state $|+\rangle = (|\downarrow\rangle + |\uparrow\rangle)/\sqrt{2}$ by a Hadamard gate. (ii) The information of the characteristic function is encoded into the auxiliary qubit by a simulated unitary operator U_t^S (see e.g., Fig. 2(a) and Fig. 3(a) respectively for the detection of magnetization order parameter and kink number). (iii) The real and imaginary parts of the characteristic function are detected by $\langle \hat{\sigma}_x \rangle$ and $\langle \hat{\sigma}_y \rangle$ respectively.

for Pauli matrices). The classical spin system is prepared in the canonical thermal equilibrium state ρ_{th} .

Step 2: The evolution of the composite system is generated by $U_t^S = \exp(-iH_{\text{int}}t)$ with $H_{\text{int}} = \epsilon \hat{\sigma}_z X$ (ϵ denotes a coupling constant), which can be further written in an explicit form as

$$U_t^S = e^{-it\epsilon \hat{\sigma}_z} \prod_{\{n_1, \dots, n_l\}} \exp(-itb\epsilon \hat{\sigma}_z \sigma_{n_1} \cdots \sigma_{n_l}). \quad (9)$$

Then, the time-evolved state reads

$$\rho_t = \frac{1}{2} (e^{i\Omega t} |\downarrow\rangle + |\uparrow\rangle) (e^{-i\Omega t} \langle\downarrow| + \langle\uparrow|) \rho_{\text{th}}, \quad (10)$$

where $\Omega = 2\epsilon X$.

Step 3: The coherence of the probe spin measured by monitoring the operator $2\hat{\sigma}_+ = \hat{\sigma}_x + i\hat{\sigma}_y$, i.e.,

$$\langle \hat{\sigma}_x \rangle + i \langle \hat{\sigma}_y \rangle = \sum_{\{\sigma_n=\pm 1\}} e^{i\Omega t} \rho_{\text{th}} = e^{i2\epsilon a t} \frac{Z(\tilde{\mathcal{J}}', \tilde{h}', \beta)}{Z(\mathcal{J}, h, \beta)}, \quad (11)$$

where $Z(\tilde{\mathcal{J}}', \tilde{h}', \beta) = \sum_{\{\sigma=\pm 1\}} e^{-\beta H_s(\mathcal{J}, h)} e^{i2\epsilon t(X-a)}$. Parameters $\tilde{\mathcal{J}}'$ and \tilde{h}' represent the effectively complex spin coupling constants and the complex magnetic field, respectively, which are dependent on the specific choice of X . If we select $2\epsilon t = \theta$, we have $\tilde{\mathcal{J}}' = \tilde{\mathcal{J}}$ and $\tilde{h}' = \tilde{h}$. Then Eq. (11) is exactly the same as the characteristic function in Eq. (8). After performing the Fourier transformation, the full distribution of X can be immediately reconstructed.

In what follows we illustrate the above general scheme by analyzing two instances of X : the magnetization M and kink number K for a finite-temperature Ising chain.

Example 1: Measuring the full distribution of the order parameter.— Let us consider the Ising chain with nearest neighbour interactions described by the Hamiltonian

$$H_s(J, h) = -J \sum_{n=1}^N \sigma_n \sigma_{n+1} - h \sum_{n=1}^N \sigma_n, \quad (12)$$

with the periodic boundary condition $\sigma_{N+1} = \sigma_1$. The analytically-continued partition function can be derived by the method of transfer matrix [31], which yields

$$Z(J, h, \beta) = \lambda_-^N + \lambda_+^N, \quad (13)$$

where $\lambda_{\pm} = e^{\beta J} \cosh(\beta h) \pm e^{-\beta J} \sqrt{1 + e^{4\beta J} \sinh^2(\beta h)}$. The magnetization, Eq. (2), is the order parameter. To determine its full distribution, we note that the numerator of the characteristic function Eq. (8) can be written as $Z(J, \tilde{h}, \beta)$, where $\tilde{h} = h + i\theta/\beta$ is the complex magnetic field.

The cumulant generating function of the magnetization, which is the logarithm of the characteristic function, admits the following expansion

$$\log F(\theta) = \sum_{j=1}^{\infty} \kappa_j \frac{(i\theta)^j}{j!}. \quad (14)$$

In the large N limit, one can invoke the approximation $Z(J, \tilde{h}, \beta) \approx \lambda_+^N(\theta)$. Explicit computation yields the following expressions for the first few cumulants (related to the mean, variance, and skewness)

$$\kappa_1 = \langle M \rangle = Nu^{-1} e^{2\beta J} \sinh(\beta h), \quad (15)$$

$$\kappa_2 = \text{Var}(M) = Nu^{-3} e^{2\beta J} \cosh(\beta h), \quad (16)$$

$$\kappa_3 = \text{Skew}(M) \kappa_2^{3/2} = Nu^{-5} v e^{2\beta J} \sinh(\beta h), \quad (17)$$

the first two being well known (see e.g. [31]), where $u = \sqrt{1 + e^{4\beta J} \sinh^2(\beta h)}$ and $v = 1 - e^{4\beta J} [2 + \cosh(\beta h)]$ for short. The finiteness of κ_q with $q > 2$ makes $P(m)$ manifestly non-normal. In the large N limit, all cumulants of $P(m)$ scale linearly with the system size N . As a result, the ratio between the amplitude of the fluctuations quantified by the root mean square $\Delta M = \kappa_2^{1/2}$ and the average magnetization per spin $\langle M \rangle$ is proportional to $\Delta M / \langle M \rangle \propto N^{-1/2}$ and fluctuations are suppressed in the thermodynamic limit. Keeping κ_1 and κ_2 and ignoring higher-order cumulants, the probability distribution can then be approximated by a Gaussian $P(m) = C \exp[-(m - \langle M \rangle)^2 / (2\text{Var}(M))]$, with support on $M \in [-N, N]$, with C a normalization constant. Deviations from this limit are manifested for nonzero values of h .

To measure the characteristic function, we use the general scheme introduced above with the unitary

$$U_t^S = \prod_{n=1}^N \exp(-it\epsilon \hat{\sigma}_z \sigma_n), \quad (18)$$

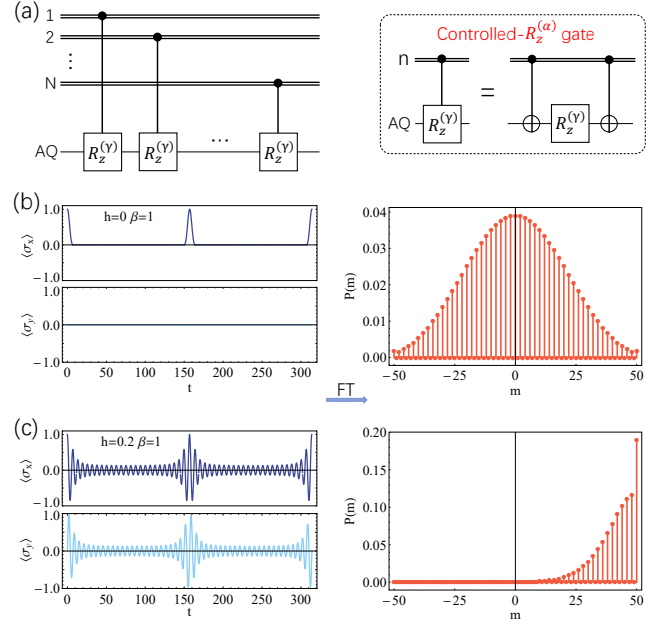


FIG. 2. Probing the distribution of the magnetization order parameter in a nearest-neighbor Ising chain. (a) A schematic quantum circuit for simulating the evolution of the composite system $U_t^S = \prod_{n=1}^N \exp(-it\epsilon \hat{\sigma}_z \sigma_n)$ [Eq. (18)]. The kernel of U_t^S is realized by a controlled- $R_z^{(\gamma)}$ gate ($\gamma = 2\epsilon t$), with $R_z^{(\alpha)} = \exp(-i\frac{\alpha}{2} \hat{\sigma}_z)$. The characteristic function of the magnetization distribution is detected by the coherence function of an auxiliary qubit. For an Ising chain of $N = 50$ spins at inverse temperature $\beta = 1$ with magnetic field (b) $h = 0$ and (c) $h = 0.2$, the real ($\langle \hat{\sigma}_x \rangle$) and imaginary ($\langle \hat{\sigma}_y \rangle$) parts of the coherence function are displayed as a function of time $t \in [0, \pi/\epsilon]$, with the spin-qubit coupling $\epsilon = 0.01$. The right panels of (b) and (c) correspond to the probability distribution of the magnetization obtained by Fourier transform (FT) of the characteristic function.

which can be simulated with quantum logical circuit depicted in Fig. 2(a). After measuring the real and imaginary parts of the coherence function of the auxiliary qubit, and performing the Fourier transformation, the distribution $P(m)$ is obtained. See examples with $h = 0$ and $h = 0.2$ in Fig. 2(b) and (c), respectively. Note that the magnetization varies in jumps of two units. For an even number of spins N , $P(m) = 0$ for odd m , while for odd N , $P(m) = 0$ for even m . We notice that our approach can be readily applied to long-range spin systems as shown in the Supplemental Material [38].

Example 2: Measuring the full kink-number distribution.— In spin systems, kinks are localized at the interface between adjacent domains. We next consider the distribution of the number of kinks. Considering Eq. (3), the corresponding complex parameters in the analytically-continued partition function in the numerator of Eq. (8) are given by $\tilde{J} = J - \frac{i\theta}{2\beta}$, and $\tilde{h} = h$.

The logarithm of the characteristic function of the kink-number distribution is the corresponding cumulant generating function. For the nearest-neighbor Ising model, approximating the partition function in the large N limit by the largest eigenvalue $Z(\tilde{J}, h, \beta) \approx \lambda_+^N(\theta)$, one finds the first cumulant, that equals the mean number of kinks

$$\langle K \rangle = \frac{N}{u\lambda_+ e^{\beta J}}. \quad (19)$$

At zero field, $h = 0$, this expression reduces to $\langle K \rangle = N/(1 + e^{2\beta J})$, which varies from 0 to $N/2$ as the temperature is increased. The explicit expression for the variance is given by

$$\text{Var}(K) = \frac{N [\cosh(\beta h) + 2e^{3\beta J} \sinh^2(\beta h) \lambda_+]}{u^3 \lambda_+^2}, \quad (20)$$

which reduces to $Ne^{2\beta J}(1 + e^{2\beta J})^{-2}$ when $h = 0$. While higher cumulants can be found making use of the expansion (14) with the corresponding characteristic function their expression becomes increasingly cumbersome (see e.g. the skewness κ_3 in [38]). At zero magnetic field, the standard deviation $\Delta K = \sqrt{\text{Var}(K)}$ over the mean vanishes as one approaches the thermodynamic limit with with increasing system size N as

$$\frac{\Delta K}{\langle K \rangle} = \frac{e^{\beta J}}{\sqrt{N}}, \quad (21)$$

and $P(k)$ approaches the normal distribution.

The general scheme can be used to experimentally determine the characteristic function, choosing

$$U_t^S = e^{-it\frac{N}{2}\epsilon\hat{\sigma}_z} \prod_{n=1}^N \exp\left(it\frac{\epsilon}{2}\hat{\sigma}_z\sigma_n\sigma_{n+1}\right), \quad (22)$$

which can be simulated with quantum logical circuit shown in Fig. 3(a). For different values of h and β , monitoring the coherence of the qubit allows one to reconstruct the full kink-number distribution $P(k)$. Non-normal features of $P(k)$ arising from nonvanishing cumulants κ_q with $q > 2$ become apparent at finite values of the magnetic field, see Figs 3(b)-(c), as well as low temperatures.

Discussions.— The scheme for probing the full distributions of magnetization and kink number in quantum systems is similar to the classical case. Assume the auxiliary qubit and the quantum spin system are initially prepared in state $|+\rangle\langle+| \otimes \rho$, where ρ is an arbitrary quantum state of the system, e.g., in or out of equilibrium. A Hadamard gate is applied to the auxiliary qubit after performing a controlled gate $X_c = |\uparrow\rangle\langle\uparrow| \otimes \exp(i\theta X) + |\downarrow\rangle\langle\downarrow| \otimes \mathbb{I}$ on the whole system. The state of the auxiliary qubit is then given by $\text{tr}_{\text{spins}}[(H \otimes \mathbb{I})X_c(|+\rangle\langle+| \otimes \rho)X_c^\dagger(H \otimes \mathbb{I})] = [\mathbb{I} + \hat{\sigma}_z \text{Re}F(\theta) - i\hat{\sigma}_y \text{Im}F(\theta)]/2$. The real

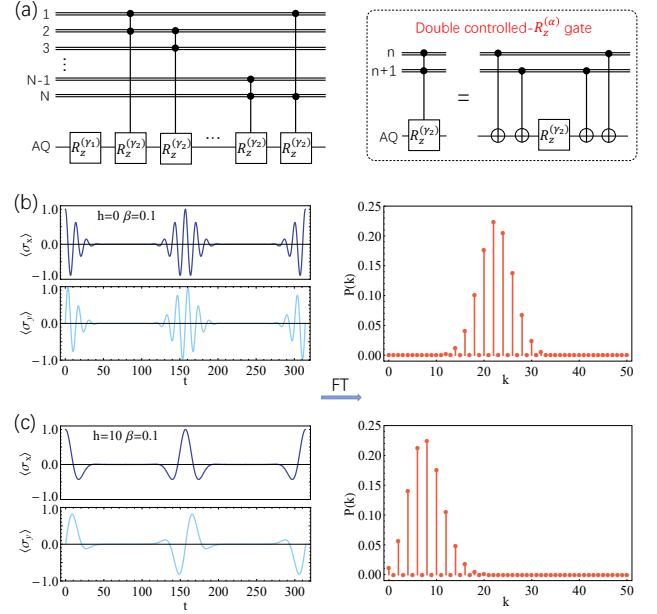


FIG. 3. **Probing the distribution of the kink number in a nearest-neighbor Ising chain.** (a) A schematic quantum circuit for simulating the evolution of the composite system $U_t^S = e^{-it\frac{N}{2}\epsilon\hat{\sigma}_z} \prod_{n=1}^N \exp(it\frac{\epsilon}{2}\hat{\sigma}_z\sigma_n\sigma_{n+1})$ [Eq. (22)], with $\gamma_1 = N\epsilon t$ and $\gamma_2 = -\epsilon t$. The real ($\langle \hat{\sigma}_x \rangle$) and imaginary ($\langle \hat{\sigma}_y \rangle$) parts of the coherence function are displayed as a function of time $t \in [0, \pi/\epsilon]$, with the spin-qubit coupling $\epsilon = 0.01$, $N = 50$, $\beta = 0.1$ and magnetic field $h = 0$ in (b) and $h = 10$ in (c). The right parts of (b) and (c) are the probability distribution of the kink number.

and imaginary parts of the characteristic thus function $F(\theta)$ can be recovered by measuring the operators $\hat{\sigma}_z$ and $\hat{\sigma}_y$, respectively, on the auxiliary qubit. See [38] for an alternative scheme. While the experimental protocol applies directly to quantum systems, the equilibrium relation between $F(\theta)$ and the analytically-continued partition function is generally lost as the system Hamiltonian H and X do not necessarily commute. Similarly, for nonequilibrium states, whether quantum or classical, the measurement protocol applies but the connection with the partition function is lost.

Summary.— We have presented a general scheme to experimentally measure the full distribution of the many-body observables in classical and quantum systems, using an auxiliary qubit as a probe. We have demonstrated our scheme by considering the distribution of the magnetization and the number of kinks in classical spin systems. In this setting, the characteristic functions of the corresponding equilibrium distributions have been shown to be directly given by the analytic continuation of the partition function. This connection is readily applicable to other spin systems where the partition function in the presence of a magnetic field is at reach, such as Heisenberg spin chains [39, 40]. We note that the ana-

lytic continuation of the partition function has already been measured experimentally in the determination of Lee-Yang zeroes in a NMR setting [29]. Our proposal is thus at reached with current technology. While we have focused on the determination of the magnetization and kink-number distributions at equilibrium, we emphasize that our scheme can be also applied to scenarios away from equilibrium. Our findings should therefore find broad applications in the characterization of many-body spin systems across different disciplines, including statistical mechanics, condensed matter or magnetometry.

Acknowledgment.— It is a pleasure to acknowledge discussions with Fernando Javier Gómez-Ruiz, Luis Pedro García-Pintos, Kohei Kawabata, and Masahito Ueda. Funding support from the John Templeton Foundation, UMass Boston (project P20150000029279), and the National Natural Science Foundation of China (Grant No. 11674238) is further acknowledged.

-
- [1] K. Binder, *Zeitschrift für Physik B Condensed Matter* **43**, 119 (1981).
 - [2] A. D. Bruce, *Journal of Physics C: Solid State Physics* **14**, 3667 (1981).
 - [3] A. D. Bruce, *Journal of Physics A: Mathematical and General* **18**, L873 (1985).
 - [4] D. Nicolaides and A. D. Bruce, *Journal of Physics A: Mathematical and General* **21**, 233 (1988).
 - [5] A. D. Bruce and N. B. Wilding, *Phys. Rev. Lett.* **68**, 193 (1992).
 - [6] S. T. Bramwell, P. C. W. Holdsworth, and J.-F. Pinton, *Nature* **396**, 552 (1998).
 - [7] V. Aji and N. Goldenfeld, *Phys. Rev. Lett.* **86**, 1007 (2001).
 - [8] T. Shinjo, *Nanomagnetism and Spintronics-Second Edition* (Elsevier, 2013).
 - [9] S. I. Denisov and P. Hänggi, *Phys. Rev. E* **71**, 046137 (2005).
 - [10] A. del Campo and W. H. Zurek, *International Journal of Modern Physics A* **29**, 1430018 (2014).
 - [11] A. del Campo, *Phys. Rev. Lett.* **121**, 200601 (2018).
 - [12] A. Recati, P. O. Fedichev, W. Zwerger, J. von Delft, and P. Zoller, *Phys. Rev. Lett.* **94**, 040404 (2005).
 - [13] D. Hangleiter, M. T. Mitchison, T. H. Johnson, M. Bruderer, M. B. Plenio, and D. Jaksch, *Phys. Rev. A* **91**, 013611 (2015).
 - [14] T. J. Elliott and T. H. Johnson, *Phys. Rev. A* **93**, 043612 (2016).
 - [15] H. T. Quan, Z. Song, X. F. Liu, P. Zanardi, and C. P. Sun, *Phys. Rev. Lett.* **96**, 140604 (2006).
 - [16] J. Zhang, X. Peng, N. Rajendran, and D. Suter, *Phys. Rev. Lett.* **100**, 100501 (2008).
 - [17] J. Goold, T. Fogarty, N. Lo Gullo, M. Paternostro, and T. Busch, *Phys. Rev. A* **84**, 063632 (2011).
 - [18] M. Knap, A. Shashi, Y. Nishida, A. Imambekov, D. A. Abanin, and E. Demler, *Phys. Rev. X* **2**, 041020 (2012).
 - [19] B. Damski, H. T. Quan, and W. H. Zurek, *Phys. Rev. A* **83**, 062104 (2011).
 - [20] R. Dorner, S. R. Clark, L. Heaney, R. Fazio, J. Goold, and V. Vedral, *Phys. Rev. Lett.* **110**, 230601 (2013).
 - [21] L. Mazzola, G. De Chiara, and M. Paternostro, *Phys. Rev. Lett.* **110**, 230602 (2013).
 - [22] A. J. Roncaglia, F. Cerisola, and J. P. Paz, *Phys. Rev. Lett.* **113**, 250601 (2014).
 - [23] T. B. Batalhão, A. M. Souza, L. Mazzola, R. Auccaise, R. S. Sarthour, I. S. Oliveira, J. Goold, G. De Chiara, M. Paternostro, and R. M. Serra, *Phys. Rev. Lett.* **113**, 140601 (2014).
 - [24] L. A. Correa, M. Mehboudi, G. Adesso, and A. Sanpera, *Phys. Rev. Lett.* **114**, 220405 (2015).
 - [25] B. Swingle, G. Bentsen, M. Schleier-Smith, and P. Hayden, *Phys. Rev. A* **94**, 040302 (2016).
 - [26] L. García-Álvarez, I. L. Egusquiza, L. Lamata, A. del Campo, J. Sonner, and E. Solano, *Phys. Rev. Lett.* **119**, 040501 (2017).
 - [27] B.-B. Wei and R.-B. Liu, *Phys. Rev. Lett.* **109**, 185701 (2012).
 - [28] B.-B. Wei, S.-W. Chen, H.-C. Po, and R.-B. Liu, *Sci. Rep.* **4**, 5202 (2014).
 - [29] X. Peng, H. Zhou, B.-B. Wei, J. Cui, J. Du, and R.-B. Liu, *Phys. Rev. Lett.* **114**, 010601 (2015).
 - [30] N. Goldenfeld, *Lectures On Phase Transitions And The Renormalization Group* (Addison-Wesley, 1992).
 - [31] M. Plischke and B. Bergersen, *Equilibrium Statistical Physics*, 2nd ed. (World Scientific, 2006).
 - [32] C. N. Yang and T. D. Lee, *Phys. Rev.* **87**, 404 (1952).
 - [33] T. D. Lee and C. N. Yang, *Phys. Rev.* **87**, 410 (1952).
 - [34] J. S. Cotler, G. Gur-Ari, M. Hanada, J. Polchinski, P. Saad, S. H. Shenker, D. Stanford, A. Streicher, and M. Tezuka, *Journal of High Energy Physics* **2017**, 118 (2017).
 - [35] E. Dyer and G. Gur-Ari, *Journal of High Energy Physics* **2017**, 75 (2017).
 - [36] A. del Campo, J. Molina-Vilaplana, and J. Sonner, *Phys. Rev. D* **95**, 126008 (2017).
 - [37] A. Chenu, I. L. Egusquiza, J. Molina-Vilaplana, and A. del Campo, *Scientific Reports* **8**, 12634 (2018).
 - [38] See *Supplemental Material*.
 - [39] M. E. Fisher, *American Journal of Physics* **32**, 343 (1964).
 - [40] P. J. Cregg, J. L. García-Palacios, and P. Svedlindh, *Journal of Physics A: Mathematical and Theoretical* **41**, 435202 (2008).

HIGHER CUMULANTS FOR THE DISTRIBUTION OF KINK NUMBER IN THE ISING CHAIN

As noted in the main text, the characteristic function $F(\theta)$ of the kink distribution $P(k)$ is given by the analytic continuation of the partition function

$$F(\theta) = Z(\tilde{J}, h, \beta) = \lambda_-^N + \lambda_+^N, \quad (23)$$

with $\tilde{J} = J - \frac{i\theta}{2\beta}$. Using a cumulant expansion, one can readily find an arbitrary cumulant. The exact first cumulant ($h = 0$) reads

$$\langle K \rangle = \frac{N}{2} e^{-\beta J} \frac{\cosh^{N-1}(\beta J) - \sinh^{N-1}(\beta J)}{\cosh^N(\beta J) + \sinh^N(\beta J)}. \quad (24)$$

The exact expressions of higher order cumulants are somewhat cumbersome. Using the simplified expression for the partition function $Z(\tilde{J}, h, \beta) \approx \lambda_+^N(\theta)$, the cumulants admit simpler expressions (see e.g. κ_1 and κ_2 in the main text). In particular, the third cumulant, which is proportional to the skewness, reads

$$\kappa_3 = \text{Skew}(K) \kappa_2^{3/2} = \frac{N e^{-\beta J} [5e^{2\beta J} - (2+w)e^{2\beta J} \cosh(2\beta h) - 2uw \cosh(\beta h) + 4(u^2 - 1)\lambda_- e^{\beta J} \cosh(\beta h)]}{2u^5 \lambda_+^3}, \quad (25)$$

where $w = 1 - 8e^{8\beta J} \sinh^4(\beta h)$.

One readily finds that the cumulant generating function is proportional to the system size, as $\log F(\theta) \approx N \log \lambda_+^N(\theta)$, where $\lambda_+^N(\theta)$ is independent of N . Thus, all cumulants of the distribution scale linearly with N .

PROBING MAGNETIZATION ORDER PARAMETER AND KINK NUMBER IN LONG-RANGE ISING CHAIN

The quantum circuit for the simulation of U_t^S is only dependent on the statistical quantity we are going to measure, but independent of the specific spin system under study, i.e., it is not specific of the short-range Ising chain. As such, it can be applied to the characterization of the distribution of many-body observables in other experimentally relevant spin systems. Let us consider the long-range Ising model, with the following Hamiltonian

$$H_s(J, h) = -J \sum_{m < n}^N \sigma_m \sigma_n - h \sum_{n=1}^N \sigma_n, \quad (26)$$

involving all-to-all pairwise interactions of equal strength. This model arises naturally in an NMR setting [29]. The corresponding partition function is given by

$$Z(J, h, \beta) = e^{\frac{N(N-1)\beta J}{2}} e^{N\beta h} \sum_{n=0}^N \binom{N}{n} e^{-2\beta h n} e^{2\beta J(n^2 - Nn)}. \quad (27)$$

In what follows we discuss the experimental protocol to characterize both the magnetization and kink-number distributions in this system.

1. Probing the probabilistic distribution of magnetization order parameter

The characteristic function of the magnetization distribution $P(m)$ can be written as

$$F(\theta) = \frac{Z(J, h + \frac{i\theta}{\beta}, \beta)}{Z(J, h, \beta)}, \quad (28)$$

which admits the explicit form

$$F(\theta) = \frac{e^{iN\theta} \sum_{n=0}^N e^{-2in\theta} g(n)}{\sum_{n=0}^N g(n)}, \quad (29)$$

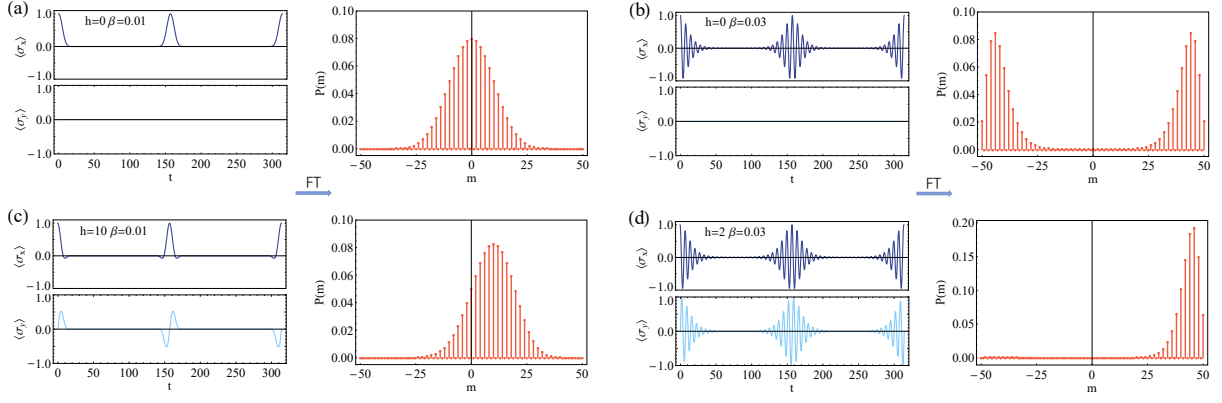


FIG. 4. **Distribution of the magnetization in a long-range Ising model.** The real ($\langle \hat{\sigma}_x \rangle$) and imaginary ($\langle \hat{\sigma}_y \rangle$) parts of the coherence function of the auxiliary qubit are detected as a function of time $t \in [0, \pi/\epsilon]$, with spin number $N = 50$, the spin-qubit coupling $\epsilon = 0.01$, and inverse temperature $\beta = 0.01$ when the magnetic field (a) $h = 0$ and (c) $h = 10$; $\beta = 0.03$ when the magnetic field (b) $h = 0$ and (d) $h = 2$. The probability distribution function $P(m)$ is constructed by performing the Fourier transformation.

where $g(n) = \binom{N}{n} e^{-2\beta hn} e^{2\beta J(n^2 - Nn)}$. Use of the cumulant expansion readily yields the first few cumulants of $P(m)$

$$\kappa_1 = \langle M \rangle = N - \frac{2G_1(N)}{G_0(N)}, \quad (30)$$

$$\kappa_2 = \text{Var}(M) = 4 \left[\frac{G_2(N)}{G_0(N)} - \left(\frac{G_1(N)}{G_0(N)} \right)^2 \right], \quad (31)$$

$$\kappa_3 = \text{Skew}(M) \kappa_2^{3/2} = -8 \left[\frac{G_3(N)}{G_0(N)} - 3 \frac{G_1(N)G_2(N)}{G_0(N)^2} + 2 \left(\frac{G_1(N)}{G_0(N)} \right)^3 \right], \quad (32)$$

where $G_\alpha(N) = \sum_{n=1}^N n^\alpha g(n)$.

The experimental proposal for probing the characteristic function is similar to *Example 1* in the main text, with numerical simulations shown in Fig. (4).

2. Probing the probabilistic distribution of kink number

The characteristic function is given by

$$F(\theta) = e^{i \frac{N\theta}{2}} \frac{Z(\tilde{\mathcal{J}}, h, \beta)}{Z(J, h, \beta)}, \quad (33)$$

where

$$\tilde{\mathcal{J}} = \begin{cases} J & n \neq m+1 \\ J - \frac{i\theta}{2\beta} & n = m+1 \end{cases} \quad (34)$$

The experimental proposal for probing the characteristic function is similar to *Example 2* in the main text, with numerical simulations shown in Fig. (5).

PROBING THE MAGNETIZATION DISTRIBUTION VIA LOSCHMIDT ECHO FOR QUANTUM SPIN SYSTEMS

We have seen that the characteristic function of the magnetization is related to the analytic continuation of the partition function. In quantum systems, the later can be measured in a variety of quantum platforms including quantum simulators of spin systems and NMR experiments. Given a Hamiltonian H with eigenvalues E_n and

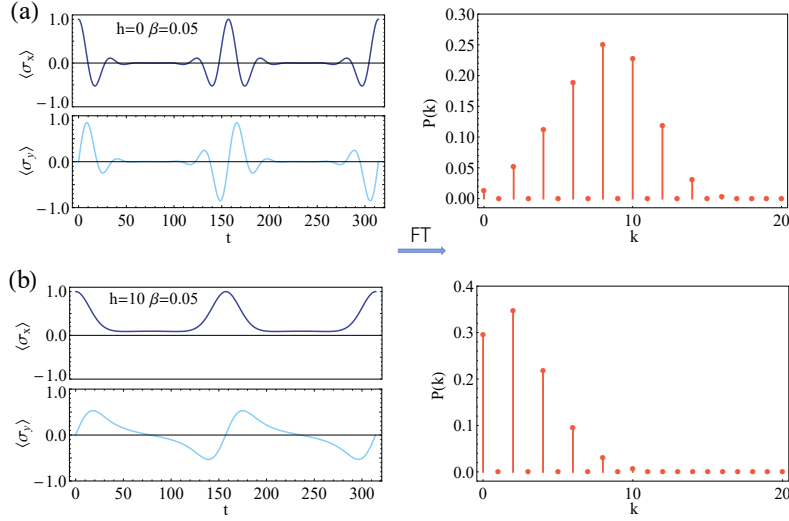


FIG. 5. **Distribution of the kink number in a long-range Ising model.** The real ($\langle\hat{\sigma}_x\rangle$) and imaginary ($\langle\hat{\sigma}_y\rangle$) parts of the coherence function of the auxiliary qubit are displayed as a function of time $t \in [0, \pi/\epsilon]$, with spin number $N = 20$, the spin-qubit coupling $\epsilon = 0.01$, inverse temperature $\beta = 0.05$, and the magnetic field (a) $h = 0$ and (b) $h = 10$. The probability distribution function $P(k)$ is shown after Fourier transformation.

energy eigenstates $|n\rangle$, the state of the system can be initialized in the coherent quantum superposition of the form $|\psi(0)\rangle = \sum_n \sqrt{p_n} |n\rangle$ where $p_n = \exp(-\beta E_n)/Z(\beta)$ and $Z(\beta) = \sum_n \exp(-\beta E_n)$ denotes the partition function. This superposition evolves into $|\psi(t)\rangle = \sum_n \exp[-(\beta/2 + it)E_n] |n\rangle / \sqrt{Z(\beta)}$, and the survival amplitude reads $\langle\psi(0)|\psi(t)\rangle = Z(\beta + it)/Z(\beta)$. Choosing as a Hamiltonian the Ising chain, the survival amplitude can be written as $\langle\psi(0)|\psi(t)\rangle = Z(\beta, h - it/\beta)/Z(\beta, h)$, this is, in terms of the analytically continued partition function for an Ising chain with a complex-valued magnetic field, and can be measured experimentally via a Loschmidt echo [29]. Its Fourier transform directly yields the full distribution of the magnetization.